UC Irvine
UC Irvine Previously Published Works

Title

miR-2940-1 is involved in the circadian regulation of oviposition in Aedes albopictus

Permalink

https://escholarship.org/uc/item/36d0x0dx

Authors

Xiao, Xiaolin

Kong, Ling

Xie, Zhensheng

et al.

Publication Date

2024-03-31

DOI

10.1111/1744-7917.13362

Peer reviewed

ORIGINAL ARTICLE

miR-2940-1 is involved in the circadian regulation of oviposition in *Aedes albopictus*

Xiaolin Xiao[1,#], Ling Kong[1,#], Zhensheng Xie[1], Hongkai Liu[1], Lijun Cai[1], Siyu Zhao[1], Jiayong Zhou[1], Shuang Liu[1], Jing Wu[1], Yiming Wu[1], Peilin Wu[1], Anthony A. James[2,3] and Xiao-Guang Chen[1]

[1]*Department of Pathogen Biology, Institute of Tropical Medicine, School of Public Health, Southern Medical University, Guangzhou, China;* [2]*Department of Microbiology & Molecular Genetics, University of California, Irvine, CA, USA and* [3]*Department of Molecular Biology & Biochemistry, University of California, Irvine, CA, USA*

Abstract The vast majority of all global species have circadian rhythm cycles that allow them to adapt to natural environments. These regular rhythms are regulated by core clock genes and recent studies have also implicated roles for microRNAs in this regulation. Oviposition is an important circadian behavior in the reproductive cycle of insect vectors of diseases, and little is known about the rhythm or its regulation in mosquitoes. *Aedes albopictus* is a diurnal mosquito that transmits arboviruses and is the major cause of outbreaks of dengue fever in China. We analyzed the oviposition rhythm patterns of *A. albopictus* under different light/dark conditions and show that the mosquitoes have an oviposition peak between zeitgeber time 9 (ZT 9) and ZT 12. Furthermore, the antagomir-mediated knockdown of expression of the microRNA *miR-2940-1* affected the oviposition rhythm of *A. albopictus*. These data support the conclusion that *miR-2940-1* is involved in the regulation of oviposition rhythm in *A. albopictus* and provide a foundation for using oviposition rhythms as a new target for vector mosquito control.

Key words *Aedes albopictus*; *miR-2940-1*; oviposition rhythm; regulation

Introduction

Global seasonal and circadian environmental changes are a direct result of the earth revolving around the sun and its axis (Patke *et al.*, 2020). Organisms have been selected to adapt to these seasonal and daily environmental changes, and the evolution of physiological and behavioral circadian rhythm cycles appears ubiquitous. Circadian cycles are characterized by activity oscillations with periodicities of approximately 24 h (Patke *et al.*, 2020). These rhythms are maintained and regulated by "biological clocks" comprising 3 components:

Correspondence: Xiao-Guang Chen, Department of Pathogen Biology, Institute of Tropical Medicine, School of Public Health, Southern Medical University, Bayi Rd, Baiyun, Guangzhou, Guangdong, 510515, China. Email: xgchen@smu.edu.cn
#These authors contributed equally to this work.

an input, a central oscillator and an output (Young, 2000; Kojima *et al.*, 2011). The central oscillator is the core of the biological clock and is composed of clock-controlled genes (CCGs) and the proteins they encode (Young, 2000; Takahashi, 2017). Stimuli from environmental cues with regular periodicity, zeitgeber, are transmitted to the central oscillator through the input. The cues entrain the endogenous self-maintaining rhythms to synchronize physiological and behavioral activities with the environment (Hastings *et al.*, 2003). The disruption of the circadian rhythm can cause a variety of pathological changes (Yu & Weaver, 2011; Roenneberg & Merrow, 2016).

The vinegar fly, *Drosophila melanogaster*, has been the focus of study of the genetic and molecular mechanisms of circadian rhythms. Core clock genes, including *period* (*per*), *clock* (*clk*), *timeless* (*tim*) and *cycle* (*cyc*), have been identified in this insect, and their expression products form interlocked transcription–translation feedback

1

loops (TTFLs) to drive their rhythmic expression (Al-lada, 2003; Yildirim *et al.*, 2022). In the first feedback loop, heterodimers comprising CLK and CYC proteins activate transcription of suppressor *per* and *tim* products by binding to the E-box enhancer elements, which make the PER/TIM heterodimers accumulate and migrate into nuclei and, in turn, suppress their own transcription. In the second feedback loop, CLK/CYC heterodimers drive the transcription of *vrille* (*vri*) and *PAR domain protein 1ε* (*Pdp1ε*), and their protein products act as a suppressor and activator, respectively, to regulate the transcription of *clk* and other CCGs (Blau & Young, 1999; Cyran *et al.*, 2003).

In addition to the regulation of core clock genes in the feedback loops, post-transcriptional regulation also plays an important role. microRNAs are a class of small, single-stranded, non-coding RNAs with lengths ranging from 18 to 24 nucleotides (nt) and are found in a wide variety of organisms, including bacteria, plants and animals. microRNA coding sequences are located in intergenic regions and in introns of mRNA-encoding genes. Through complementarity-based binding to the target mRNA "seed sequence", which is either in the 3′ untranslated region (UTR) or open reading frame (ORF), miRNAs can lead to the degradation or inhibition of translation of the target transcript (Wightman *et al.*, 1993; Bartel, 2004; Ørom *et al.*, 2008; Legeai *et al.*, 2010). Previous studies have shown a role for miRNAs in modulating the oscillation cycle, amplitude, phase and other aspects of circadian rhythms (Xue & Zhang, 2018). Some miRNAs target core clock genes to affect their rhythmic expression to achieve regulation of the circadian rhythms (Dubruille *et al.*, 2009; Kadener *et al.*, 2009; Garaulet *et al.*, 2016; Niu *et al.*, 2019; Xia *et al.*, 2020).

The Asian tiger mosquito, *Aedes albopictus*, is a highly adaptable species found in a wide range of habitats throughout tropical, subtropical and some temperate regions of the world (Lwande *et al.*, 2020). It is one of 100 species demonstrating the most rapid global spread during the past 20 years (Li *et al.*, 2018; Pichler *et al.*, 2018). It is an important vector of insect-borne infectious diseases and can transmit at least 26 pathogenic viruses, including dengue virus, yellow fever virus and Zika virus (Kampango & Abílio, 2016). Oviposition is an essential part of all mosquito life histories, enabling population stability. We monitored the oviposition rhythm in *A. albopictus* and used miRNA antagonism technology to study its molecular regulatory mechanisms. These data provide the potential to develop novel vector control technologies based on the suppression of mosquito reproduction.

Materials and methods

Mosquito strains

The *A. albopictus* wild-type (WT) Foshan strain was collected from Foshan, Guangdong Province, in 1981 and supplied by the Center for Disease Prevention and Control (CDC), Guangdong Province, China. Larvae were reared in standard insectary conditions at 28 ± 1 °C, 80% ± 5% relative humidity and a 14 h light/10 h dark (14/10 LD) photoperiod. Pupae and adults were reared at the same temperature and relative humidity with a 12/12 LD photoperiod. The 12/12 LD cycle was achieved with lights on at zeitgeber time 0 (ZT 0) (8:00 a.m.) and lights off at ZT 12 (20:00 p.m.). Larvae were reared in stainless-steel trays containing dechlorinated water, which was replaced after 1−2 d, and were provided with yeast and turtle food. Pupae were collected and separated individually into 2 mL Eppendorf tubes with 1 mL of dechlorinated water. Emergent adults were placed in mosquito cages (20 cm × 20 cm × 30 cm) in an artificial climate chamber at ratios of 1 : 3 females to males and provided with 10% glucose solution *ad libitum*. At 5 d post emergence, females were fed on the blood of healthy Kunming mice to trigger the production of eggs.

Oviposition rhythm analysis

Peak oviposition days following a blood meal were determined for subsequent experiments. Female mosquitoes were blood fed at 5:30−7:00 p.m., which is close to the peak biting period observed in *A. albopictus* in the laboratory (Muhammad *et al.*, 2020). Females fed to repletion were separated and allowed to digest the bloodmeal for 1 d after feeding. Oviposition cups (a 300 mL transparent plastic cup with 100 mL of dechlorinated water and a wetted filter paper cone) were provided at ZT 0 on the second day post feeding and were replaced once daily at the same time. Egg papers were transferred to moist conditions and the eggs allowed to develop until they turned from white to black and were visible to the naked eye. The number of eggs was recorded daily until the day 7 post feeding, at which time the frequency of deposition and the number of eggs laid were significantly lower.

The oviposition peak experiments revealed that females of *A. albopictus* laid the most eggs on day 3 after a blood meal, and we used this as the date for the follow-up experiment. According to the experimental requirements, 1 d after emergence adult mosquitoes were

placed in an artificial climate chamber with different day and night light cycles, and 40 female mosquitoes were mated in a 1 : 3 ratio with 120 male mosquitoes. The 12/12 LD cycle has "lights on" at ZT 0 (8:00 a.m.) and "lights off" at ZT 12 (20:00 p.m.). The 12/12 DL cycle has that "lights on" at ZT 12 (20:00 p.m.) and "lights off" at ZT 0 (8:00 a.m.). The mosquitoes were synchronized and mated freely under LD or DL conditions for 5 d, and blood was supplied between 5:30 an 7:00 p.m. on the last day. After 2 h of blood feeding, 30 female mosquitoes fed to repletion were selected and placed in an artificial climate box and allowed to digest the blood for 2 d. In the continuous darkness (DD) and DL experiments used to verify whether the oviposition rhythm is endogenous or regulated by light, we changed the light to DD (LDDD or DLDD) after a blood meal under LD or DL conditions. After blood meal digestion and egg development for 3 d under the above light conditions (4 d to test forced egg holding), an oviposition cup was placed in the chamber at 8:00 a.m. on days 3 or 4 after the blood meal and was replaced successively every 3 h (ZT/CT 0, 3, 6, 9, 12, 15, 18, 21 and 24), and again after 24 h (for the antagonism test at 48 h), and the number of eggs laid was recorded for each time period (Fig. 1A).

RNA isolation and quantitative real-time PCR analysis

Total RNA from heads, carcasses (bodies without heads) or whole bodies of 15 mated non-blood-fed or blood-fed female mosquitoes, raised under the LD photoperiod, was isolated at 5 d post emergence (PE) with TRIzol Reagent (Invitrogen, Carlsbad, CA, USA) at ZT 0, 3, 6, 9, 12, 15, 18, 21 and 24. Genomic DNA in the RNA samples was removed using the TURBO DNA-free Kit (Invitrogen). RNA quantity and quality were determined with a NanoDrop 2000 spectrophotometer (Thermo Fisher Scientific, Waltham, MA, USA). First-strand cDNA was synthesized with GoScript Reverse Transcription System (Promega, Madison, WI, USA) following the manufacturer's instructions. Quantitative real-time PCR (qPCR) was performed with gene-specific primers (Table S1) using the SYBR Selected Master Mix (Applied Biosystems, Foster City, CA, USA) under the following conditions: 50 °C for 2 min, 95 °C for 2 min, 40 cycles of 15 s at 95 °C, 15 s at 60 °C and a final extension at 72 °C for 1 min with a LightCycle96 Instrument (Roche Diagnostics, Indianapolis, IN, USA). *U6* gene transcripts were used as an endogenous control for miRNA. Each treatment was replicated 3 times and abundance levels were calculated using the $2^{-\triangle\triangle Ct}$ method (Livak & Schmittgen, 2001).

miRNA expression oscillation analysis

miRDeep2 was used to identify and quantify microRNA (miRNA) accumulation from small RNA-seq data, and the JTK_CYCLE algorithm was used to detect rhythmic miRNAs (Hughes *et al.*, 2010; Friedländer *et al.*, 2012). Initially, raw sequencing reads were subjected to quality control checks using FastQC 0.12 (Andrews, 2014). Subsequently, adapter sequences were trimmed using Cutadapt 4.6 (Martin, 2011), and reads shorter than 18 nt were discarded. The high-quality reads were then aligned with the reference genome using the mapper module of miRDeep2. The miRDeep2 core algorithm was employed to identify known and novel miRNAs, and to quantify their expression. The JTK_CYCLE algorithm, a non-parametric statistical algorithm, was used to identify miRNAs exhibiting rhythmic accumulation profiles with default parameters. The targets of miRNA were predicted using RNAhybrid (Krüger & Rehmsmeier, 2006), miranda (Enright *et al.*, 2003) and targetscan (Agarwal *et al.*, 2018), and we retained all genes that were commonly predicted by these tools. Gene ontology enrichment analysis was conducted using the clusterProfiler package with default parameters (Wu *et al.*, 2021). All statistical analyses were conducted in the R environment (The R Foundation for Statistical Computing, Vienna Austria).

Antagomir and negative control injection treatment

The *miR-2940-1* antagomir, 5′-(mA)* (mG)* (mU) (mG) (mA) (mU) (mU) (mU) (mA) (mU) (mC) (mU) (mC) (mC) (mC) (mU) (mG) (mU) (mC)* (mG)* (mA)* (mC)*-3′, and the antagomir negative control, 5′-(mA)* (mG)* (mU) (mG) (mA) (mU) (mU) (mU) (mA) (mU) (mC) (mU) (mC) (mC) (mC) (mU) (mG) (mU) (mC)* (mG)* (mA)* (mC)*-3′, designed and purchased from Sangon Biotech (Shanghai, China), were utilized to assess the function of *miR-2940-1*. Female mosquitoes were cold-anesthetized and injected intrathoracically with 1 μL of 30 μmol/L *miR-2940-1* antagomir. Mosquitoes were allowed to recover for 48 h after injection and were then provided with a blood meal.

Statistical analysis

All data were analyzed using one-way analysis of variance (ANOVA) and the Student's *t*-test analysis program of SPSS 25.0 (IBM, Armonk, NY, USA), and mean data are shown as mean ± SEM. The statistical computations and graph plotting were performed using Prism 8
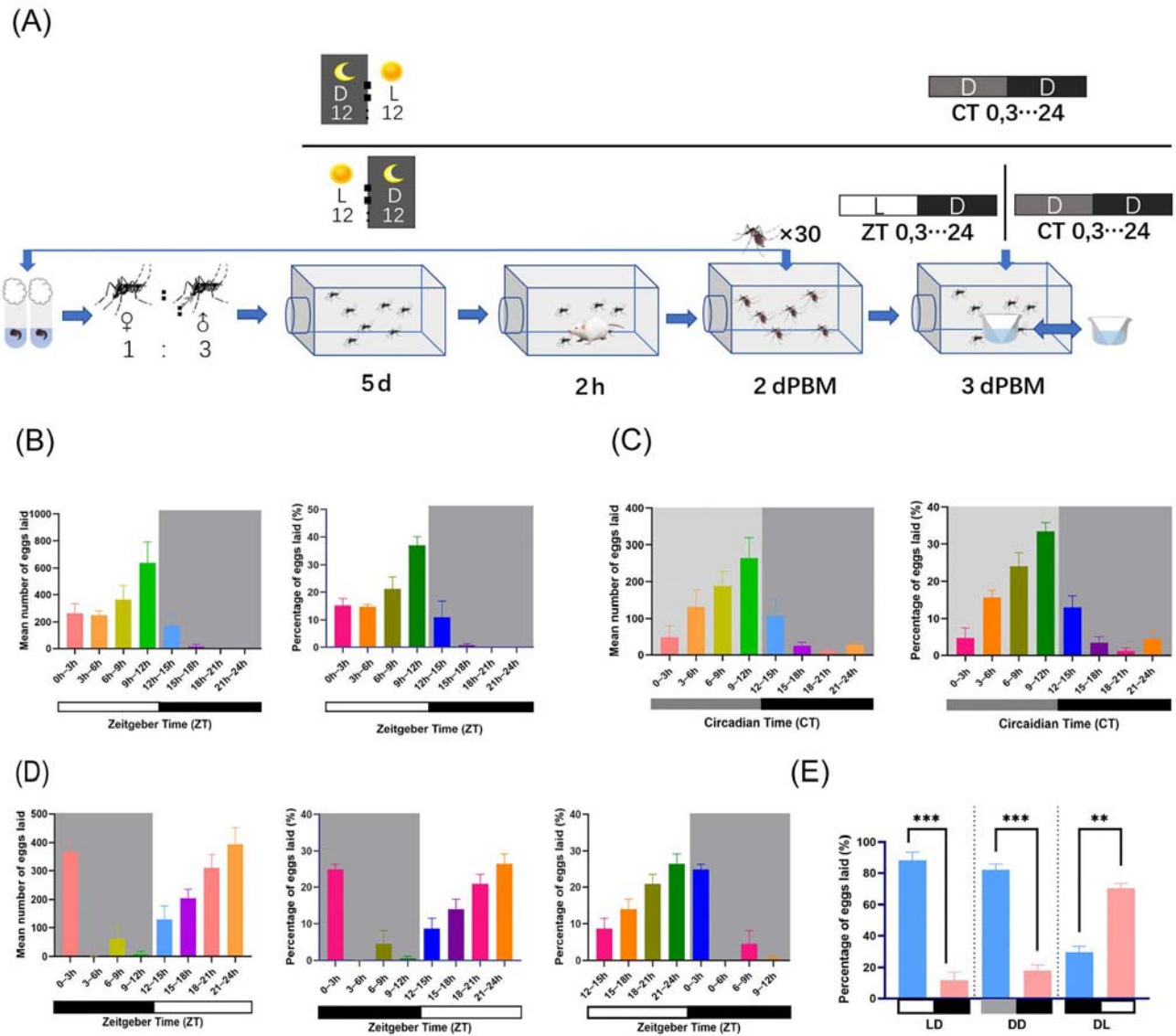
Fig. 1 Oviposition rhythms in *Aedes albopictus*. (A) Experimental flow chart of oviposition rhythm trials in *A. albopictus*. ZT, zeitgeber time; CT, circadian time. (B−D) The number and proportion of eggs laid by females ($n = 30$) 3 d post blood meal (dPBM) at 3 h intervals for 24 h under LD conditions (B), under DD conditions (C) and under DL conditions (D). (E) Circadian comparison of oviposition activity. The normalized value is expressed as the mean $\pm$ standard error of the mean (SEM), and *P* values were calculated using one-way analysis of variance (ANOVA) and the Student's *t*-test. **P < 0.01, ***P < 0.001.

(GraphPad, San Diego, CA, USA). $P < 0.05$ was considered to be statistically significant.

Results

Oviposition rhythm in A. albopictus

The peak period of oviposition under LD conditions was determined for use in subsequent experiments. The number of eggs laid increased on the second day post

blood meal (dPBM), peaked at 3 dPBM and then declined rapidly (Fig. S1). The average number of eggs deposited at 3 dPBM accounted for 69.1% of the total number of eggs laid (Fig. S1; Table S2).

The 3 dPBM time point was chosen as the day for the experiments to determine oviposition rhythms (Fig. 1A). The diel oviposition activity and number of eggs laid exhibited a unimodal circadian rhythm ($P < 0.0001$) under LD conditions, with a peak at ZT 9−ZT 12 (peak ZT 9−ZT 12 vs trough ZT 18−ZT 24, $P < 0.001$) (Fig. 1B; Table S3). In addition, the diel oviposition

activity was higher during the day (lights on, ZT 0−ZT 12, 88.2%; Table S3) than at night (lights off, ZT 12−ZT 24, 11.8%, *P* < 0.001; Fig. 1E; Table S3).

The results of experiments conducted under DD conditions to determine whether the rhythm was controlled by an endogenous clock were similar to those under LD conditions, demonstrating a unimodal circadian oscillation (*P* < 0.0001), with significant (*P* < 0.001) differences between peak (CT 9−CT 12) and trough (CT 18−CT 21) values (Fig. 1C; Table S4). The diel oviposition activity of subjective daytime (time when lights should be on, CT 0−CT 12, 77.8%; Table S4) was higher than that of subjective nighttime (time when lights should be off, CT 12−CT 24, 22.2%; Table S4) (*P* < 0.001, Fig. 1E).

The times for the light and dark periods were then reversed for DL conditions to explore whether the rhythm is regulated by the zeitgeber of light (Fig. 1D). Diel oviposition activity appeared entrained by DL conditions, and still showed a unimodal circadian oscillation (*P* < 0.0001) with a statistically significant (*P* < 0.001) difference between the peak (ZT 21−ZT 24) and the trough (ZT 3−ZT 6) periods. Interestingly, the diel oviposition activity changed correspondingly with the reversal of the artificial light and darkness regimens, with the activity during the subjective daytime (ZT 12−ZT 24, 70.1%; Table S5) being higher than that during the subjective nighttime (ZT 0−ZT 12, 29.9%; Table S5) (*P* < 0.01), whereas the oviposition peak is the same as that under LD and DD conditions for ZT 21−ZT 24 (26.5%; Fig. 1E; Table S5).

The impact of delayed access to oviposition sites on oviposition rhythm was evaluated by forcing females to retain eggs up to 4 dPBM under LD conditions (Fig. S2). Unimodal circadian oscillations (*P* < 0.001) were observed, with a significant difference between peak (ZT 6−ZT 9) and trough (ZT 15−ZT 24) values (*P* < 0.01). The diel oviposition activity was also higher during the daytime (90.9%) than at nighttime (9.1%) (*P* < 0.0001; Fig. S2; Table S6). However, in contrast to the results at 3 dPBM, the peak in oviposition occurred at ZT 6−ZT 9 (30.7%; Table S6), which was earlier than previously observed (Fig. S2). Altogether, these results support the conclusion that *A. albopictus* exhibits oviposition rhythms that are controlled by an endogenous clock, regulated by the zeitgeber of light, and not impaired by access to oviposition sites.

Characterization of miR-2940-1 in A. albopictus

Previous analyses of RNA-seq data identified 9 miRNAs, including *miR-2940-1*, with oscillating abundance

profiles in *A. albopictus* (Fig. S3). The likely *miR-2940-1* ortholog, *miR-2940-3p*, in *Aedes aegypti*, was shown to affect the development of eggs in this species (Aksoy & Raikhel, 2021). Moreover, the gene ontology enrichment analysis revealed numerous terms associated with embryo development and oviposition, including embryonic morphogenesis, eggshell formation and embryo development, ending in birth or egg hatching, among others (Table S7). We posited that *miR-2940-1* may have a role in the regulation of oviposition rhythm in *A. albopictus*.

Analysis of the *miR-2940-1* abundance profile using reverse transcription (RT) qPCR was performed using female tissue samples collected at ZT 0, 3, 6, 9, 12, 15, 18, 21 and 24, using ZT 0 as the control group (Fig. 2A). *miR-2940-1* abundance in the head showed an obvious and significant circadian oscillation (*P* < 0.001), with a peak at ZT 15 and a trough at ZT 3, and with the difference being statistically significant (*P* < 0.01). The abundance profile of the body also had a circadian rhythm oscillation (*P* < 0.0001), with a peak at ZT 12 and a trough at ZT 6 (*P* < 0.001). The peak abundance in the body occurred earlier than that of the head and, correspondingly, the lowest abundance in the head was earlier than that of the body. The head and body oscillations confirmed the results of previous RNA-seq analysis.

Samples of *miR-2940-1* were collected at different time points from 3 dPBM and the abundance profile was determined using RT-qPCR (Fig. 2B). The abundance profile showed an obvious and significant circadian oscillation (*P* < 0.05), with a statistically significant (*P* < 0.05) difference in the peak at ZT 18 and the trough at ZT 9. Evaluated in the context of the rhythm of oviposition, the decreased relative abundance levels of *miR-2940-1* at ZT 0−ZT 9 correspond with increased daytime oviposition activity at ZT 0−ZT 12, and the peak in oviposition activity at ZT 9−ZT 12 corresponds with the low abundance of *miR-2940-1* at ZT 9. The subsequent increase in the abundance of *miR-2940-1* at ZT 12−ZT 24 also correlated with a decrease in the percentage of eggs laid at ZT 12−ZT 24.

The knockdown of miR-2940-1 affects A. albopictus oviposition rhythms

The previous analyses support a possible role for *miR-2940-1* in regulating oviposition rhythm in *A. albopictus*. Antagomirs were used to disrupt *miR-2940-1* function and test this hypothesis. An antagomir with a randomly-disrupted *miR-2940-1* sequence served as a negative control. The optimal concentration of antagomirs for injection was determined using a concentration gradient
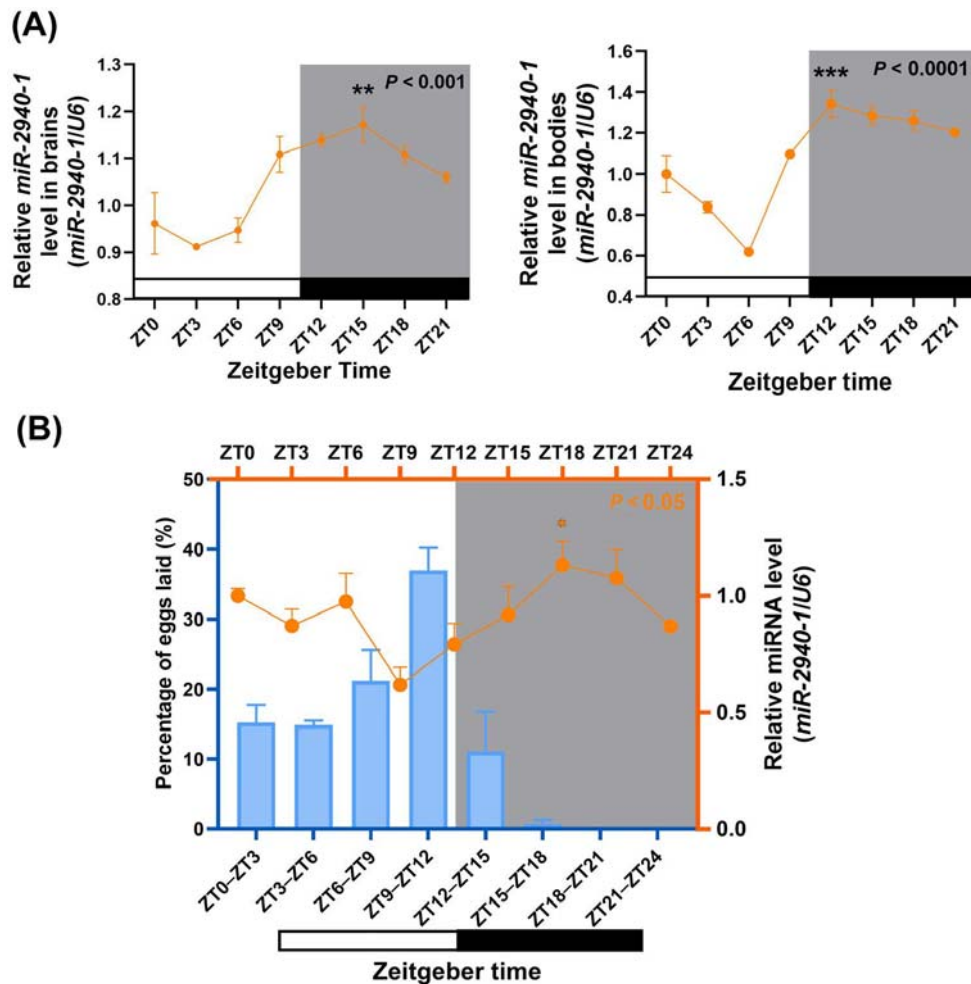
Fig. 2 Abundance profiles of *miR-2940-1* in *Aedes albopictus*. (A) Abundance profiles of *miR-2940-1* from the head and body of female mosquitoes ($n = 15$) raised under LD conditions. **$P < 0.01$ and ***$P < 0.001$ indicate significant differences between the relative abundance levels at ZT 15 and ZT 3, and at ZT 12 and ZT 6, respectively. (B) Comparison of oviposition rhythm and *miR-2940-1* abundance profiles at 3 d post blood meal (dPBM) under LD conditions. *$P < 0.05$ indicates a significant difference between the relative abundance levels at ZT 18 and ZT 9. The *U6* gene was used as the reference gene. The normalized value is expressed as the mean ± SEM, and *P* values were calculated using one-way analysis of variance (ANOVA) and the Student's *t*-test.

(Fig. S4). Using uninjected mosquitoes as a negative control, injections of 4 antagomir concentrations, 10, 20, 30 and 50 μmol/L, resulted in significant reductions in *miR-2940-1* abundance ($P < 0.0001$). Injection with 30 μmol/L antagomir solution decreased the abundance by an average of 92.5%, whereas injection with the 50 μmol/L solution resulted in a 94.1% reduction. As mosquito mortality after the injection was higher with the 50 μmol/L solution, the 30 μmol/L solution was used in all subsequent experiments. The duration of the antagomir effect after injection was measured to calibrate the efficacy in subsequent experiments (Fig. S4). There was no significant difference in the abundance of *miR-*

2940-1 daily between the uninjected and negative control samples at 5 d post injection (dPI) ($P > 0.05$), so the negative control could be used and the antagomir still demonstrated an antagonistic effect at this time point.

Three groups of 20 female mosquitoes each (at 1 dPBM) were injected intrathoracically with 30 μmol/L *miR-2940-1* as the experimental group, with control antagomirs as the negative control or were left uninjected as the WT control. These mosquitoes were reared under LD conditions for 3 dPI and then their respective oviposition rhythms were assayed. Negative control values were comparable with those of the WT (uninjected) and the mosquitoes demonstrate an oviposition rhythm
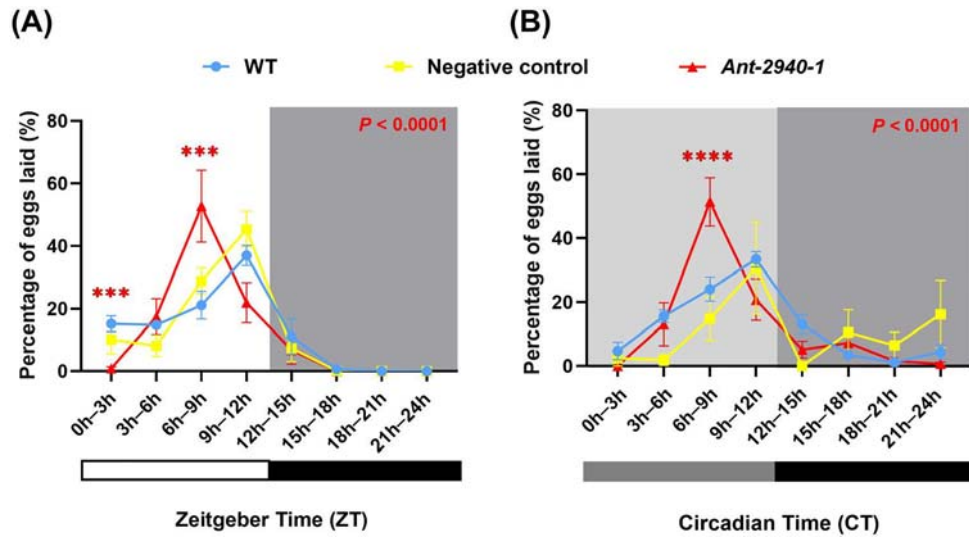
Fig. 3 Oviposition rhythms following injection with *miR-2940-1* antagomirs and negative control. Effects of injection with 1 μL of 30 μmol/L *miR-2940-1* antagomir, or negative control, after 5 d of synchronous activity under LD and DD conditions in female *Aedes albopictus* ($n = 20$), compared with WT ($n = 30$) oviposition rhythms. (A) Comparison of oviposition rhythms following injection of antagomir and negative control with WT under LD conditions. ***$P < 0.001$ indicates that the percentage of eggs laid after injection with *Ant-2940-1* significantly differed from that of WT at ZT 0−ZT 3 and ZT 6−ZT 9. (B) Comparison of oviposition rhythms following injection of antagomir and negative control with that of the WT under DD conditions. ****$P < 0.0001$ indicates that the percentage of eggs laid after injection with *Ant-2940-1* differed significantly at CT 6−CT 9. The normalized value is expressed as the mean $\pm$ SEM and P values were calculated using the one-way analysis of variance (ANOVA) and the Student's *t*-test.

($P < 0.0001$, Fig. 3A). Female mosquitoes treated with the antagomir *Ant-2940-1* showed unimodal oviposition rhythms consistent with those of the WT and those treated with the negative control ($P < 0.0001$; Fig. 3A), with peak activity at ZT 6−ZT 9 and with the lowest activity at ZT 15−ZT 24 ($P < 0.001$). The proportion of eggs oviposited and the activity during the daytime (93.2%) were both higher than during the nighttime (6.8%, $P < 0.01$; Table S8). However, there were significant differences in the phase of the oviposition peak (ZT 6−ZT 9, 52.8%; Table S8), compared with ZT 9−ZT 12 in the WT and the negative control. At the same time, the oviposition activity and percentage of eggs laid at ZT 0−ZT 3 decreased significantly ($P < 0.001$), and there were no significant alterations in the oscillation patterns, amplitudes or other parameters.

We also analyzed mosquitoes raised under DD conditions and the results showed that the negative control had no effect (Fig. 3B). However, female mosquitoes still had a unimodal oviposition rhythm following injection with the antagomir ($P < 0.0001$; Fig. 3B), with a significant difference between peak CT 6−CT 9 and trough CT 15−CT 24 values ($P < 0.0001$). Furthermore, the proportion of eggs and activity level during the subjective daytime (85.2%; Table S9) were higher than during

the subjective nighttime (14.8%, $P < 0.0001$; Table S9). However, the oviposition peak had a significant advance in phase (CT 6−CT 9, 51.4%, Table S9) compared with the WT and the negative control, which is consistent with the shift seen under LD conditions.

Discussion

We describe here the oviposition rhythm patterns in female *A. albopictus* following a blood meal and a potential regulatory role of miRNA in this circadian behavior. Oviposition falls into the group of regulated circadian activities, which include locomotor activity (Mandilaras & Missirlis, 2012; Weiss *et al.*, 2014; Kijak & Pyza, 2017), mating (Liu *et al.*, 2022), host seeking and biting (Muhammad *et al.*, 2020), feeding (Dreyer *et al.*, 2019) and olfactory activity (Krishnan *et al.*, 1999). Oviposition rhythms exist in other insects, including: the vinegar fly, *D. melanogaster* (Howlader *et al.*, 2006); queens of the honey bee, *Apis mellifera* (Shpigler *et al.*, 2022); crickets, *Gryllus bimaculatus* (Itoh & Sumi, 2000); and locusts, *Schistocerca gregaria* (Newland & Yates, 2007). Using different light-cycle conditions, *A. albopictus* oviposition activity was found to be concentrated mainly during the

daytime, which is expected of a mosquito with diurnal locomotor activity (Kawada *et al.*, 2005; George *et al.*, 2015; Baik *et al.*, 2020). Our results are comparable with previous reports of unimodal, twilight-phase oviposition in *A. albopictus* (Chadee & Corbet, 1989). Wild *A. albopictus* females also deposited eggs rhythmically, and the number of eggs laid during the daytime (peaking in the afternoon) was significantly higher than during the nighttime (Trexler *et al.*, 1997). However, although the rhythm of locomotor activity is bimodal under standard LD conditions, oviposition rhythms are unimodal. In addition, the oviposition peak was at ZT 9−ZT 12, with more daytime and less nighttime activity, but the morning and evening activity peaks were after the lights were switched on (ZT 0) and before the lights were switched off (ZT 12), respectively (Feitoza *et al.*, 2020). Thus, the oviposition peak activity occurs just before lights off, a pattern also seen in *A. aegypti* (Wong *et al.*, 2011).

The oviposition activity under LD conditions after the forced retention of eggs (with no oviposition sites provided) was also rhythmic, which supports the conclusion that rhythmic oscillations are regulated by circadian clocks and not by a strict regimen of development. The peak in oviposition occurred earlier, which may be attributed to the expansion and pressure on the female abdomen while holding their eggs (Chadee, 2010). Under DD (LDDD) conditions, without light entrainment, the oviposition activity still had a rhythm, likely regulated endogenously. In addition, under DL (DLDD) conditions, with the opposite light cycle to that found in nature, the oviposition activity also showed rhythmicity in accordance with the light cycle, proving that the oviposition rhythm is regulated by the zeitgeber of light.

In previous studies of circadian RNA abundance profiles in *A. aegypti* and in our RNA-seq work in *A. albopictus*, we posited that microRNAs, specifically *miR-2940-1* in *A. albopictus*, may have a role in regulating oviposition activity (Aksoy & Raikhel, 2021). Our studies show that the accumulation profiles of *miR-2940-1* in the heads and bodies of *A. albopictus*, with peak values during the night and with lowest values during the day, support the hypothesis that they have self-sustaining oscillators, that is, local clock oscillations exist in the central brain tissue and in peripheral tissue (Yoo *et al.*, 2004; Kornmann *et al.*, 2007). Studies of *miR-375* (Xia *et al.*, 2020), *miR-263a*, *miR-263b* (Yang *et al.*, 2008) and *miR-276a* (Zhang *et al.*, 2021) revealed that they all oscillated in the heads of *D. melanogaster*, and had different regulatory effects on the circadian rhythm. In contrast, other studies have shown that circadian oscillation of mature miRNAs may not be necessary to regulate circadian rhythms (Gatfield *et al.*, 2009; Chen *et al.*, 2013).

Based on the correlation between the abundance profile of *miR-2940-1* after a blood meal and oviposition rhythm, we looked for an effect of *miR-2940-1* on oviposition rhythm. There is only one report, and none in insects, of a clock-controlled *miR-449c-5p* regulating egg production, through modulating Ca^{2+} transport in the chicken uterus by targeting ATP2B4 during eggshell calcification (Cui *et al.*, 2021). Following the injection of *miR-2940-1* into *A. albopictus* females, the phase of the oviposition peak was advanced, whereas the period ZT 0−ZT 3 or CT 0−CT 3 demonstrated no oviposition activity. However, which genes *miR-2940-1* targets to regulate oviposition rhythm remains to be determined.

Our report successfully defines patterns of oviposition rhythms in *A. albopictus*, and by studying the potential regulatory impact of the miRNAs on oviposition rhythm, provides a basis for the precise application of relevant insecticides and attractants in the future, as well as the use of the miRNAs as new targets for biological control strategies of vector mosquitoes.

Acknowledgments

Disclosure

The authors have declared that they have no competing interests associated with this work.

References

Agarwal, V., Subtelny, A.O., Thiru, P., Ulitsky, I. and Bartel, D.P. (2018) Predicting microRNA targeting efficacy in *Drosophila*. *Genome Biology*, 19, 152.

Aksoy, E. and Raikhel, A.S. (2021) Juvenile hormone regulation of microRNAs is mediated by E75 in the Dengue vector mosquito *Aedes aegypti*. *Proceedings of the National Academy of Sciences USA*, 118, e2102851118.

Allada, R. (2003) Circadian clocks: a tale of two feedback loops. *Cell*, 112, 284–286.

Andrews, S. (2014) FastQC: a quality control tool for high throughput sequence data. https://www.bioinformatics.babraham.ac.uk/projects/fastqc/

Baik, L.S., Nave, C., Au, D.D., Guda, T., Chevez, J.A., Ray, A. et al. (2020) Circadian regulation of light-evoked attraction and avoidance behaviors in daytime-versus nighttime-biting mosquitoes. *Current Biology*, 30, 3252–3259.

Bartel, D.P. (2004) MicroRNAs: genomics, biogenesis, mechanism, and function. *Cell*, 116, 281–297.

Blau, J. and Young, M.W. (1999) Cycling *vrille* expression is required for a functional *Drosophila* clock. *Cell*, 99, 661–671.

Chadee, D.D. (2010) The diel oviposition periodicity of *Aedes aegypti* (L.) (Diptera: Culicidae) in Trinidad, West Indies: effects of forced egg retention. *Bulletin of Entomological Research*, 100, 599–603.

Chadee, D.D. and Corbet, P.S. (1989) Diel pattern of oviposition in the laboratory of the mosquito *Aedes albopictus* (Skuse) (Diptera: Culicidae). *Annals of Tropical Medicine and Parasitology*, 83, 423–429.

Chen, R., D'Alessandro, M. and Lee, C. (2013) miRNAs are required for generating a time delay critical for the circadian oscillator. *Current Biology*, 23, 1959–1968.

Cui, Z., Zhang, Z., Amevor, F.K., Du, X., Li, L., Tian, Y. et al. (2021) Circadian *miR-449c-5p* regulates uterine Ca^{2+} transport during eggshell calcification in chickens. *BMC Genomics*, 22, 764.

Cyran, S.A., Buchsbaum, A.M., Reddy, K.L., Lin, M.C., Glossop, N.R., Hardin, P.E. et al. (2003) *Vrille*, *Pdp1*, and *dClock* form a second feedback loop in the *Drosophila* circadian clock. *Cell*, 112, 329–341.

Dreyer, A.P., Martin, M.M., Fulgham, C.V., Jabr, D.A., Bai, L., Beshel, J. et al. (2019) A circadian output center controlling feeding: fasting rhythms in *Drosophila*. *PLoS Genetics*, 15, e1008478.

Dubruille, R., Murad, A., Rosbash, M. and Emery, P. (2009) A constant light-genetic screen identifies KISMET as a regulator of circadian photoresponses. *PLoS Genetics*, 5, e1000787.

Enright, A.J., John, B., Gaul, U., Tuschl, T., Sander, C. and Marks, D.S. (2003) MicroRNA targets in *Drosophila*. *Genome Biology*, 5, R1.

Feitoza, T.S., Ferreira-de-Lima, V.H., Câmara, D.C.P., Honório, N.A., Lounibos, L.P. and Lima-Camara, T.N. (2020) Interspecific mating effects on locomotor activity rhythms and refractoriness of *Aedes albopictus* (Diptera: Culicidae) Females. *Insects*, 11, 874.

Friedländer, M.R., Mackowiak, S.D., Li, N., Chen, W. and Rajewsky, N. (2012) miRDeep2 accurately identifies known and hundreds of novel microRNA genes in seven animal clades. *Nucleic Acids Research*, 40, 37–52.

Garaulet, D.L., Sun, K., Li, W., Wen, J., Panzarino, A.M., O'Neil, J.L. et al. (2016) *miR-124* regulates diverse aspects of rhythmic behavior in *Drosophila*. *The Journal of Neuroscience*, 36, 3414–3421.

Gatfield, D., Le Martelot, G., Vejnar, C.E., Gerlach, D., Schaad, O., Fleury-Olela, F. et al. (2009) Integration of microRNA *miR-122* in hepatic circadian gene expression. *Genes & Development*, 23, 1313–1326.

George, K.A., Archer, M.S. and Toop, T. (2015) Correlation of molecular expression with diel rhythm of oviposition in *Calliphora vicina* (Robineau-Desvoidy) (Diptera: Calliphoridae) and implications for forensic entomology. *Journal of Forensic Sciences*, 60, S108–S115.

Hastings, M.H., Reddy, A.B. and Maywood, E.S. (2003) A clockwork web: circadian timing in brain and periphery, in health and disease. *Nature Reviews Neuroscience*, 4, 649–661.

Howlader, G., Paranjpe, D.A. and Sharma, V.K. (2006) Non-ventral lateral neuron-based, non-PDF-mediated clocks control circadian oviposition rhythm in *Drosophila melanogaster*. *Journal of Biological Rhythms*, 21, 13–20.

Hughes, M.E., Hogenesch, J.B. and Kornacker, K. (2010) JTK_CYCLE: an efficient nonparametric algorithm for detecting rhythmic components in genome-scale data sets. *Journal of Biological Rhythms*, 25, 372–380.

Itoh, M.T. and Sumi, Y. (2000) Circadian clock controlling egg hatching in the cricket (*Gryllus bimaculatus*). *Journal of Biological Rhythms*, 15, 241–245.

Kadener, S., Menet, J.S., Sugino, K., Horwich, M.D., Weissbein, U., Nawathean, P. et al. (2009) A role for microRNAs in the *Drosophila* circadian clock. *Genes & Development*, 23, 2179–2191.

Kampango, A. and Abílio, A.P. (2016) The Asian tiger hunts in Maputo city—the first confirmed report of *Aedes* (*Stegomyia*) *albopictus* (Skuse, 1895) in Mozambique. *Parasites & Vectors*, 9, 76.

Kawada, H., Takemura, S.Y., Arikawa, K. and Takagi, M. (2005) Comparative study on nocturnal behavior of *Aedes aegypti* and *Aedes albopictus*. *Journal of Medical Entomology*, 42, 312–318.

Kijak, E. and Pyza, E. (2017) TOR signaling pathway and autophagy are involved in the regulation of circadian rhythms in behavior and plasticity of L2 interneurons in the brain of *Drosophila melanogaster*. *PLoS ONE*, 12, e0171848.

Kojima, S., Shingle, D.L. and Green, C.B. (2011) Post-transcriptional control of circadian rhythms. *Journal of Cell Science*, 124, 311–320.

Kornmann, B., Schaad, O., Bujard, H., Takahashi, J.S. and Schibler, U. (2007) System-driven and oscillator-dependent circadian transcription in mice with a conditionally active liver clock. *PLoS Biology*, 5, e34.

Krishnan, B., Dryer, S.E. and Hardin, P.E. (1999) Circadian rhythms in olfactory responses of *Drosophila melanogaster*. *Nature*, 400, 375–378.

Krüger, J. and Rehmsmeier, M. (2006) RNAhybrid: microRNA target prediction easy, fast and flexible. *Nucleic Acids Research*, 34, W451–W454.

Legeai, F., Rizk, G., Walsh, T., Edwards, O., Gordon, K., Lavenier, D. *et al.* (2010) Bioinformatic prediction, deep sequencing of microRNAs and expression analysis during phenotypic plasticity in the pea aphid, *Acyrthosiphon pisum*. *BMC Genomics*, 11, 281.

Li, Y., Xu, J., Zhong, D., Zhang, H., Yang, W., Zhou, G. *et al.* (2018) Evidence for multiple-insecticide resistance in urban *Aedes albopictus* populations in southern China. *Parasites & Vectors*, 11, 4.

Liu, S., Zhou, J., Kong, L., Cai, Y., Liu, H., Xie, Z. *et al.* (2022) *Clock* genes regulate mating activity rhythms in the vector mosquitoes, *Aedes albopictus* and *Culex quinquefasciatus*. *PLoS Neglected Tropical Diseases*, 16, e0010965.

Livak, K.J. and Schmittgen, T.D. (2001) Analysis of relative gene expression data using real-time quantitative PCR and the $2^{-\Delta\Delta Ct}$ Method. *Methods (San Diego, California)*, 25, 402–408.

Lwande, O.W., Obanda, V., Lindström, A., Ahlm, C., Evander, M., Näslund, J. *et al.* (2020) Globe-trotting *Aedes aegypti* and *Aedes albopictus*: risk factors for arbovirus pandemics. *Vector Borne and Zoonotic Diseases*, 20, 71–81.

Martin, M. (2011) CUTADAPT removes adapter sequences from high-throughput sequencing reads. *EMBnet. Journal*, 17, 10–12.

Mandilaras, K. and Missirlis, F. (2012) Genes for iron metabolism influence circadian rhythms in *Drosophila melanogaster*. *Metallomics: Integrated Biometal Science*, 4, 928–936.

Muhammad, N.A.F., Abu Kassim, N.F., Ab Majid, A.H., Abd Rahman, A., Dieng, H. and Avicor, S.W. (2020) Biting rhythm and demographic attributes of *Aedes albopictus* (Skuse) females from different urbanized settings in Penang Island, Malaysia under uncontrolled laboratory conditions. *PLoS ONE*, 15, e0241688.

Newland, P.L. and Yates, P. (2007) Nitrergic modulation of an oviposition digging rhythm in locusts. *The Journal of Experimental Biology*, 210, 4448–4456.

Niu, Y., Liu, Z., Nian, X., Xu, X. and Zhang, Y. (2019) *miR-210* controls the evening phase of circadian locomotor rhythms through repression of Fasciclin 2. *PLoS Genetics*, 15, e1007655.

Ørom, U.A., Nielsen, F.C. and Lund, A.H. (2008) MicroRNA-10a binds the 5'UTR of ribosomal protein mRNAs and enhances their translation. *Molecular Cell*, 30, 460–471.

Patke, A., Young, M.W. and Axelrod, S. (2020) Molecular mechanisms and physiological importance of circadian rhythms. *Nature Reviews Molecular Cell Biology*, 21, 67–84.

Pichler, V., Bellini, R., Veronesi, R., Arnoldi, D., Rizzoli, A., Lia, R.P. *et al.* (2018) First evidence of resistance to pyrethroid insecticides in Italian *Aedes albopictus* populations 26 years after invasion. *Pest Management Science*, 74, 1319–1327.

Roenneberg, T. and Merrow, M. (2016) The circadian clock and human health. *Current Biology*, 26, R432–R443.

Shpigler, H.Y., Yaniv, A., Gernat, T., Robinson, G.E. and Bloch, G. (2022) The influences of illumination regime on oviposition rhythms of honey bee queens. *Journal of Biological Rhythms*, 37, 609–619.

Takahashi, J.S. (2017) Transcriptional architecture of the mammalian circadian clock. *Nature Reviews Genetics*, 18, 164–179.

Trexler, J.D., Apperson, C.S. and Schal, C. (1997) Diel oviposition patterns of *Aedes albopictus* (Skuse) and *Aedes triseriatus* (Say) in the laboratory and the field. *Journal of Vector Ecology: Journal of the Society for Vector Ecology*, 22, 64–70.

Weiss, R., Bartok, O., Mezan, S., Malka, Y. and Kadener, S. (2014) Synergistic interactions between the molecular and neuronal circadian networks drive robust behavioral circadian rhythms in *Drosophila melanogaster*. *PLoS Genetics*, 10, e1004252.

Wightman, B., Ha, I. and Ruvkun, G. (1993) Posttranscriptional regulation of the heterochronic gene *lin-14* by *lin-4* mediates temporal pattern formation in *C. elegans*. *Cell*, 75, 855–862.

Wong, J., Astete, H., Morrison, A.C. and Scott, T.W. (2011) Sampling considerations for designing *Aedes aegypti* (Diptera: Culicidae) oviposition studies in Iquitos, Peru: substrate preference, diurnal periodicity, and gonotrophic cycle length. *Journal of Medical Entomology*, 48, 45–52.

Wu, T., Hu, E., Xu, S., Chen, M., Guo, P., Dai, Z. *et al.* (2021) clusterProfiler 4.0: a universal enrichment tool for interpreting omics data. *The Innovation*, 2, 100141.

Xia, X., Fu, X., Du, J., Wu, B., Zhao, X., Zhu, J. *et al.* (2020) Regulation of circadian rhythm and sleep by *miR-375-timeless* interaction in *Drosophila*. *FASEB Journal*, 34, 16536–16551.

Xue, Y. and Zhang, Y. (2018) Emerging roles for microRNA in the regulation of *Drosophila* circadian clock. *BMC Neuroscience*, 19, 1.

Yang, M., Lee, J.E., Padgett, R.W. and Edery, I. (2008) Circadian regulation of a limited set of conserved microRNAs in *Drosophila*. *BMC Genomics*, 9, 83.

Yildirim, E., Curtis, R. and Hwangbo, D.S. (2022) Roles of peripheral clocks: lessons from the fly. *FEBS Letters*, 596, 263–293.

Young, M.W. (2000) Marking time for a kingdom. *Science*, 288, 451–453.

Yoo, S.H., Yamazaki, S., Lowrey, P.L., Shimomura, K., Ko, C.H., Buhr, E.D. *et al.* (2004) PERIOD2: LUCIFERASE real-time reporting of circadian dynamics reveals persistent

circadian oscillations in mouse peripheral tissues. *Proceedings of the National Academy of Sciences USA*, 101, 5339–5346.

Yu, E.A. and Weaver, D.R. (2011) Disrupting the circadian clock: gene-specific effects on aging, cancer, and other phenotypes. *Aging*, 3, 479–493.

Zhang, R., Zhao, X., Du, J., Wei, L. and Zhao, Z. (2021) Regulatory mechanism of daily sleep by *miR-276a. FASEB Journal*, 35, e21222.

Supporting Information

Additional supporting information may be found online in the Supporting Information section at the end of the article.

Fig. S1 Daily oviposition patterns in *Ae. albopictus*.

Fig. S2 Oviposition rhythm in female *Ae. albopictus* forced to retain eggs.

Fig. S3 Nine *Ae. albopictus* miRNAs accumulating with circadian rhythmicity.

Fig. S4 Screening and verification of the optimal injection concentration of *miR-2940-1* antagomir and antagonistic efficiency in *Ae. albopictus*.

Table S1 Oligonucleotide primers used in this study.

Table S2 Eggs laid per day (%) in *Aedes albopictus*.

Table S3 Eggs laid per day (%) in *Aedes albopictus* under LD conditions.

Table S4 Eggs laid per day (%) in *Aedes albopictus* under DD conditions.

Table S5 Eggs laid per day (%) in *Aedes albopictus* under DL conditions.

Table S6 Eggs laid per day (%) in *Aedes albopictus* forced to retain eggs under LD conditions.

Table S7 Gene ontology terms related to embryo development and oviposition associated with targets of *miR-2940-1*.

Table S8 List of oviposition rhythm in *Aedes albopictus* following injection of *miR-2940-1* antagomir and negative control under LD conditions.

Table S9 List of oviposition rhythm in *Aedes albopictus* following injection of *miR-2940-1* antagomir and negative control under DD conditions.